of the arm, including the cuff and the supporting beam. The right side is the torque imposed on this composite object and is the sum of muscle-generated torque (τ_{in}) and the torque applied by the PFM (τ_{ext}). τ_{in} depends nonlinearly on muscle length (a function of $\mathbf{q}$) and velocity (a function of $\dot{\mathbf{q}}$) as well as on the descending motor commands ($\mathbf{u}$). τ_{ext} can be measured by the force sensor attached to the handle of the PFM. By linearizing Eq. 1 around the unperturbed, control trajectory, the following variational equation can be derived:

$$\mathbf{I}\delta\ddot{\mathbf{q}} + \frac{\partial \mathbf{H}}{\partial \dot{\mathbf{q}}}\delta\dot{\mathbf{q}} + \left(\frac{\partial \mathbf{I}\ddot{\mathbf{q}}}{\partial \mathbf{q}} + \frac{\partial \mathbf{H}}{\partial \mathbf{q}}\right)\delta\mathbf{q} = \frac{\partial \tau_{in}}{\partial \dot{\mathbf{q}}}\delta\dot{\mathbf{q}} + \frac{\partial \tau_{in}}{\partial \mathbf{q}}\delta\mathbf{q} + \delta\tau_{ext} \equiv -\mathbf{D}\delta\dot{\mathbf{q}} - \mathbf{R}\delta\mathbf{q} + \delta\tau_{ext} \quad (2)$$

where $\delta\mathbf{q}$, $\delta\dot{\mathbf{q}}$, and $\delta\ddot{\mathbf{q}}$ are positional, velocity, and acceleration perturbations, respectively, caused by imposed force perturbation $\delta\tau_{ext}$ by the PFM. In the analysis, they were, respectively, measured as the difference between the perturbed trajectory and the control trajectory (the average of perturbed trajectories) and its first and second derivatives. Offsets in all quantities relative to the control trajectory at the start of a perturbation were eliminated. The force perturbation was derived as the difference between the perturbed and the control external torque patterns. **D** and **R** denote viscosity and stiffness matrices, respectively. If we apply a least-squared error estimation method to this variational equation, then the time-variant 2 × 2 matrices for the acceleration coefficient (inertia), velocity coefficient (viscosity), and position coefficient (stiffness) can be estimated, but for the inertial matrix 36 (4 components × 9 times), independent parameters must be estimated. Because the left sides of both Eqs. 1 and 2 can be linearized with respect to the physical parameters of the links, only three independent parameters are sufficient to specify them. Those are uniquely determined from the physical characteristics of the links. These three parameters were preestimated with the use of all the data sets measured for each person, then viscosity and stiffness were estimated at each perturbation time (*18*).

16. At least three objections might exist concerning our way of calculating the equilibrium-point trajectory. One is to assert that the nonlinear muscle length-tension curve [especially the exponentially increasing, accelerating nonlinearity (*5*)] can produce large forces even with the equilibrium-point trajectory close to the actual trajectory. Our approach, a linearization of the nonlinear length-tension curve, may overestimate the difference between the equilibrium and actual positions. By recalling that arm stiffness is measured around the actual trajectory, not around the equilibrium-point trajectory, we can actually show the opposite. Let us define the following single joint stiffness values as the derivative of τ_{in} with respect to θ but estimated at the actual position θ and the equilibrium position θ_{eq}: $R \equiv -\partial\tau_{in}(\theta)/\partial\theta$ and $R_{eq} \equiv -\partial\tau_{in}(\theta_{eq})/\partial\theta_{eq}$. From the accelerating nonlinearity of τ_{in}, we can assert that $R_{eq} < R$, and $|\tau_{in}/R| < |\theta_{eq}^{real} - \theta|$. Here, θ_{eq}^{real} denotes the real equilibrium position considering the nonlinearity of the muscle length-tension curve. The second possible criticism is a new version of the equilibrium-point control hypothesis that uses not only the position information of the desired trajectory (θ_d) but also its velocity wave form for generating muscle torque, such as $\tau_{in} = R(\theta_d - \theta) + D(\dot{\theta}_d - \dot{\theta})$ (*6*). For the case of single joint movement, it was demonstrated that with this new version a simple trajectory can control relatively fast movement (*6*). However, we found that even with this new version, a simple straight equilibrium-point trajectory cannot control multijoint movements (*10*) [N. Schweighofer, thesis, University of Southern California (1995)]. This is reasonable because the viscosity force is always one order of magnitude smaller than the elastic force in our experiments. The third possible criticism is that for some reason our measured stiffness values are different from those used under the equilibrium-point control hypothesis. For example, stiffness value estimations depend on the perturbations used. In our exploratory experiments, we found that the measured stiffness values became smaller for larger amplitude perturbations and for lower temporal frequency (*12, 13*). Because the equilibrium-point trajectory seems to be larger in amplitude and lower in temporal frequency than the currently used perturbation patterns, our stiffness estimation may be an overestimation. Consequently, our main conclusion here still holds.

17. M. Kawato, K. Furukawa, R. Suzuki, *Biol. Cybern.* **57**, 169 (1987); M. Kawato and H. Gomi, *Trends Neurosci.* **15**, 445 (1992); M. Shidara, K. Kawano, H. Gomi, M. Kawato, *Nature* **365**, 50 (1993).
18. H. Gomi and M. Kawato, *Technical Report No. ISRL-95-4* (NTT Basic Research Labs, Information Science Research Lab, 1995).

19. We thank M. Honda and K. Ishii of NTT and Y. Tohkura of ATR for their continuing encouragement; F. Pollick and S. Schaal for improving the manuscript; and N. Imamura and E. Nagaoka of KOBELCO and T. Yoshioka of CSK Corp. for their technical support. Supported by Human Frontier Science Program grants to M.K.

10 October 1995; accepted 5 February 1996

Role of the Nuclear Transport Factor p10 in Nuclear Import

Ulf Nehrbass and Günter Blobel*

The nuclear import factor p10 was cloned from *Saccharomyces cerevisiae* and found to be essential. The protein p10 can bind directly to several peptide repeat–containing nucleoporins. It also binds to the guanosine triphosphatase (GTPase) Ran in its guanosine diphosphate (GDP)–bound form and to karyopherin β. Assembly of the karyopherin heterodimer on immobilized nucleoporin yielded cooperative binding of p10 and Ran-GDP. Addition of GTP to this pentameric complex led to dissociation of karyopherin α, presumably via in situ formation of Ran-GTP from Ran-GDP. Thus, p10 appears to coordinate the Ran-dependent association and dissociation reactions underlying nuclear import.

Protein import across the nuclear pore complex (NPC) is mediated by at least four soluble factors. These cytosolic factors restore nuclear import in cells depleted of cytosol by digitonin permeabilization. Two of these factors form a heterodimer termed karyopherin (*1–9*). Karyopherin α binds to nuclear localization sequence (NLS)–containing proteins (*2, 10–12*), and karyopherin β mediates docking to peptide repeats of nucleoporins (*1, 10, 13*). The GTPase Ran (*14, 15*) and an additional protein referred to as p10 (*10, 16, 17*) are required for subsequent translocation of the docked NLS protein into the nucleoplasm (*1, 10, 14, 16*) along with karyopherin α. Karyopherin β remains bound to the NPC (*8, 10*). The role of p10 in the translocation reaction is not clear. It can bind to the nucleoporin p62 (*17*) and appears to form a complex with Ran in the cytosol (*16*), although a direct interaction has not yet been demonstrated.

Saccharomyces cerevisiae contains a conserved set of import factors (*18*). In solution-binding assays (*19*), the karyopherin αβ heterodimer (Kap60α and Kap95β) associates with either NLS protein or nucleoporin FXFG (phenylalanine-X-phenylalanine-glycine) repeats in a cooperative fashion. Moreover, Ran-GTP dissociates the heterodimeric αβ complex by binding to karyopherin β, thus releasing the karyopherins from the nucleoporin docking site. Ran-GDP binds to karyopherin β with much lower affinity and does not induce dissociation (*20*). As docking and release are principal functions of soluble factors, nuclear translocation has been proposed to result from repeated docking and release reactions along an array of docking sites on the NPC fibers (*13*). Because Ran-GTP is the major

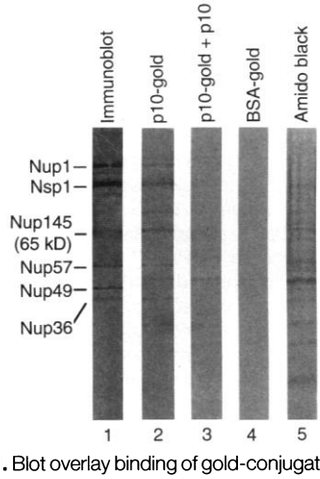

Fig. 1. Blot overlay binding of gold-conjugated p10 to a subset of nucleoporins. Proteins of yeast nuclear envelopes (*26, 28*) were separated by SDS-PAGE and transferred to nitrocellulose. The protein pattern is shown by Amido black staining (lane 5). Strips were probed with p10-gold conjugate (*27*) in the absence (lane 2) or presence (lane 3) of a 200-fold excess of nonconjugated p10, or were probed with a BSA-gold conjugate (lane 4). Another strip (lane 1) was probed with monoclonal antibodies 14 and 192 (*29*), which recognize the peptide repeat motifs of various nucleoporins, and with an affinity-purified antibody against Nup36 (*31*).

Laboratory of Cell Biology, Howard Hughes Medical Institute, Rockefeller University, New York, NY 10021, USA.

*To whom correspondence should be addressed. E-mail: blobel@rockvax.rockefeller.edu

dissociating force during these iterative dissociation and association cycles, its spatial and temporal activity must be tightly controlled for nuclear transport to proceed.

In an effort to understand the function of p10 in nuclear translocation, we cloned and sequenced the DNA for yeast p10 (*21*). The open reading frame coded for a protein 125 residues long, which is 45.6% identical to *Xenopus* p10 (*22*). Deletion of the gene encoding p10 showed it to be essential for viability (*23*). Immunofluorescence microscopy with affinity-purified mouse antibodies to recombinant p10 (*24*) showed a punctate nuclear rim staining that is characteristic for nucleoporins, with additional weak cytoplasmic and nucleoplasmic signals (*25*). To directly demonstrate binding to nucleoporins, we used overlay blotting. Proteins of a yeast nuclear envelope fraction (*26*) were separated by SDS–polyacrylamide gel electrophoresis (SDS-PAGE), transferred to nitrocellulose, and blotted with recombinant p10 coupled to gold (*27, 28*). Five major p10 binding proteins could be detected, which co-migrated with a subset of peptide repeat–containing nucleoporins (Fig. 1) (*29*). Addition of a 200-fold excess of unconjugated p10 competed for the p10-gold signal, suggesting that the p10 binding was specific. Thus, p10 binds to a subset of peptide repeat nucleoporins.

To study the individual interactions of p10 with karyopherin α or β, Ran, or the nucleoporin Nup36 [a nucleoporin that contains five FXFG peptide repeats and a COOH-terminal RanBP1 homologous domain (*24, 30, 31*)], we used a liquid phase binding assay, with p10 immobilized on Affi-Gel (Fig. 2). Nup36 bound, which is consistent with its peptide repeats (Fig. 2). Ran-GDP also bound, although Ran-GTP (*32*) did not. Moreover, karyopherin β (*32*) bound, but no karyopherin α binding was detected (Fig. 2).

The binary interactions of p10 with Ran-GDP, karyopherin β, and a subset of nucleoporins suggested that it might function in the assembly of a larger complex. To test this hypothesis, we immobilized a glutathione S-transferase (GST) fusion protein with ΔNup36 [truncated Nup36 lacking the RanBP1 homologous domain (*31*)] on glutathione agarose for use in liquid phase binding assays. A striking increase in binding of p10 and Ran-GDP to ΔNup36 could be seen in the presence of karyopherin α and β (Fig. 3), whereas binding was either very weak or not detectable when various combinations of three or fewer of the four transport factors were used (Fig. 3) (*33*). Thus, the low binding affinities between Nup36 and p10, Ran-GDP and p10, and karyopherin β and p10, as well as Ran-GDP and karyopherin β (*20*) cooperate to yield an apparently stoichiometric pentameric complex in which p10 docks Ran-GDP to nucleoporin and the karyopherin heterodimer.

If the function of p10 is to associate Ran-GDP with docked karyopherin αβ, what is the physiological importance of such a complex? Because addition of p10 and Ran to docked karyopherin αβ triggers αβ dissociation and nuclear translocation of α and NLS substrate in permeabilized cells (*1, 10, 14, 16*), we assumed that the pentameric complex resembles a short-lived intermediate stabilized by a lack of GTP. To simulate more closely the in vitro nuclear import system, we docked karyopherin α and β to ΔNup36, washed the complex, subsequently added p10 and Ran-GDP, and then incubated with GTP. We observed that 10 min after addition of GTP, most of the karyopherin α was dissociated from the complex, whereas most of the karyopherin β remained bound (Fig. 4). At the 60-min time point, karyopherin α was entirely released, although most of the karyopherin β was still bound (Fig. 4) (*34*). If GDP was added instead of GTP, karyopherin binding remained unaffected (Fig. 4). Addition of GTP-Ran led to complete dissociation of both karyopherin α and β, as reported previously (*19*). Addition of Ran-GDP and GTP in the absence of p10 led to a slight release of both karyopherin α and β in equal ratio (Fig. 4) (*35*).

The GTP-triggered partial dissociation of the pentameric complex is consistent with the functional characteristics of a nuclear import intermediate. Because only Ran-GTP is able to dissociate the karyopherin heterodimer (*19*), the release of monomeric karyopherin α must have been preceded by a GDP-GTP exchange reaction, transforming Ran-GDP into its GTP-bound

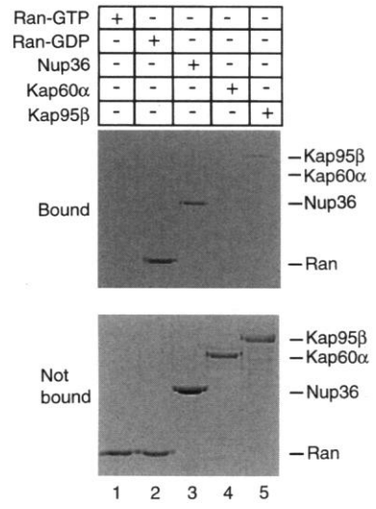

Fig. 2. Immobilized p10 binds Ran-GDP but not Ran-GTP and shows additional binding affinities to both Nup36 and karyopherin β. Recombinant p10 was immobilized to AffiGel-15 beads (8 μg per 10 μl of packed beads). Packed p10-resin (10 μl) was incubated with 3 μg each of Ran-GTP (*32*) (lane 1), Ran-GDP (*32*) (lane 2), Nup36 (*24*) (lane 3), Kap60α (lane 4), or Kap95β (lane 5) (*32*) for 30 min at 20°C. Total bound fraction and 50% of the unbound fractions were analyzed by SDS-PAGE and Coomassie staining.

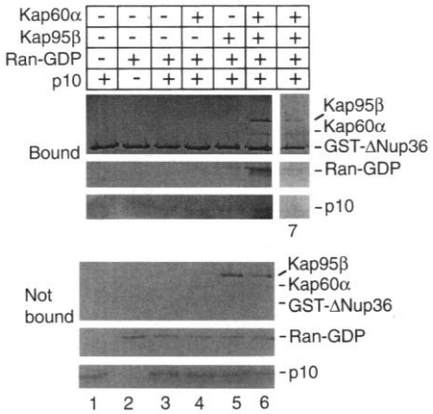

Fig. 3. p10 binds Ran-GDP to GST-ΔNup36 in the presence of the karyopherin heterodimer. GST-ΔNup36 (*24, 31*) was immobilized on glutathione agarose (2 μg per 10 μl of packed beads) and incubated for 30 min at 20°C with 2 μg of p10, 1 μg of Ran-GDP, 0.6 μg of Kap60α, or 0.6 μg of Kap95β in the indicated combinations. Fifty percent each of the total bound and unbound fractions were analyzed by SDS-PAGE and silver stain (lanes 1 through 6) or Coomassie stain (lane 7). Coomassie staining was included to show the disproportionally intense staining of Ran with silver (lane 6), as the gel containing the bound fractions was stained longer than was the gel with nonbound fractions.

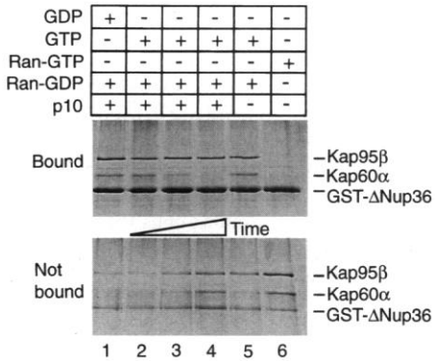

Fig. 4. Addition of p10, Ran-GDP, and GTP to prebound karyopherin heterodimer leads to release of karyopherin α. Immobilized GST-ΔNup36 was preincubated with Kap60α and Kap95β (0.6 μg of each) for 20 min at 20°C. After being washed, beads were incubated as indicated above each lane with 1 μg of Ran-GDP, 1 μg of Ran-GTP, 2 μg of p10, 200 μM GDP, or 200 μM GTP at 20°C for 1 min (lane 2) or 10 min (lane 3) or 60 min (lanes 1, 4, 5, and 6). Fifty percent each of the total bound and unbound fractions were analyzed by SDS-PAGE and silver stain.

form. The p10 requirement for the release of monomeric karyopherin α (see Fig. 4), moreover, suggests that Ran-GDP has to be part of the pentameric complex in order for exchange to occur. As karyopherin α shares sequence homology with a GDP-GTP exchange factor of Ras (*5, 36*), one possibility is that karyopherin α catalyzes a Ran–GDP-GTP exchange, thus triggering its own release from karyopherin β. It remains to be shown, however, whether the rate-limiting step of karyopherin α release is the GDP-GTP exchange or the Ran-GTP–mediated karyopherin dissociation (*19*). The retention of karyopherin β could result from cooperative interactions due to its binding affinities to FXFG repeats (*19*) and p10 (Fig. 2). Nucleoporin-bound karyopherin β is consistent with results from in vitro nuclear import experiments (*8, 10*).

The existence of a pentameric nuclear import intermediate would imply that Ran-GDP, and not Ran-GTP, is the primary active form. Conversion to Ran-GTP would be a secondary event, tightly controlled through formation of the pentameric complex. This scenario is consistent with the high cytosolic Ran-GAP (Ran-GTPase activating protein) activity that has recently been associated with the product of the yeast *RNA1* gene (*37*). If this Ran-GAP activity kept cytosolic Ran primarily in the GDP-bound form, as would be expected, association reactions both in the cytosol (NLS–α-β complex) and at the NPC (α-β–Nup complex) could proceed unantagonized by Ran-GTP. The formation of these complexes would become a mechanistic prerequisite for the in situ formation of Ran-GTP, at the very location of its requirement. Thus, by binding Ran-GDP into a complex with nucleoporin-docked karyopherins, it is likely that p10 coordinates the activity of Ran and ensures the spatial and temporal separation of association and dissociation events during nuclear import. In a nuclear import machinery that may entirely depend on iterative docking and undocking cycles, a coordinating function of p10 may well explain why mutant cells that lack p10 do not survive.

REFERENCES AND NOTES

1. A. Radu, G. Blobel, M. S. Moore, *Proc. Natl. Acad. Sci. U.S.A.* **92**, 1769 (1995).
2. J. Moroianu, G. Blobel, A. Radu, *ibid.*, p. 2008.
3. N. Imamoto, T. Tachibana, M. Matsubae, Y. Yoneda, *J. Biol. Chem.* **270**, 8859 (1995).
4. E. J. H. Adam and S. A. Adam, *J. Cell Biol.* **125**, 547 (1994).
5. D. Görlich, S. Prehn, R. Laskey, E. Hartmann, *Cell* **79**, 767 (1994).
6. N. Imamoto *et al.*, *EMBO J.* **14**, 3617 (1995).
7. D. Görlich *et al.*, *Curr. Biol.* **5**, 383 (1995).
8. D. Görlich *et al.*, *Nature* **377**, 246 (1995).
9. N. C. Chi, E. J. H. Adam, S. A. Adam, *J. Cell Biol.* **130**, 265 (1995).
10. J. Moroianu, M. Hijikata, G. Blobel, A. Radu, *Proc. Natl. Acad. Sci. U.S.A.* **92**, 6532 (1995).
11. S. A. Adam and L. Gerace, *Cell* **66**, 837 (1991).
12. K. Weis, I. Mattaj, A. Lamond, *Science* **268**, 1049 (1995).
13. A. Radu, M. S. Moore, G. Blobel, *Cell* **81**, 215 (1995).
14. M. S. Moore and G. Blobel, *Nature* **365**, 661 (1993).
15. F. Melchior, J. Paschal, J. Evans, L. Gerace, *J. Cell Biol.* **123**, 1649 (1993).
16. M. S. Moore and G. Blobel, *Proc. Natl. Acad. Sci. U.S.A.* **91**, 10212 (1994).
17. B. M. Paschal and L. Gerace, *J. Cell Biol.* **129**, 925 (1995).
18. C. Enenkel, G. Blobel, M. Rexach, *J. Biol. Chem.* **270**, 16499 (1995).
19. M. Rexach and G. Blobel, *Cell* **83**, 683 (1995).
20. M. Floer and G. Blobel, *J. Biol. Chem.* **271**, 1 (1996).
21. The yeast p10 gene was cloned out of a yeast genomic library probed with a random prime ^{32}P-labeled DNA fragment amplified by polymerase chain reaction (PCR) corresponding to amino acids 1 to 53 of a partial open reading frame from *S. cerevisiae* (GenBank accession number P33331). The full-length gene has meanwhile been sequenced by the yeast genome sequencing project (GenBank accession number 603601).
22. Sequences were compared pairwise with the use of the Wilbur-Lipman method, which showed 45.6% identity between yeast and *Xenopus* p10 genes.
23. The deletion of the p10 gene in strain W303 (*38*) was performed by integrative transformation with the use of the procedure of Rothstein (*39*), with modifications as described (*38*).
24. To obtain recombinant p10, Nup36, or GST-ΔNup36 (*29*), corresponding genes were amplified with PCR primers carrying a 5′ flanking Bam HI site substituting for the initiation codon ATG and a 3′ Eco RI site. The further subcloning, expression, and protein purification steps were performed as described (*18*).
25. Indirect immunofluorescence was performed after 5 min of fixation of yeast spheroplasts in 3.7% formaldehyde as described elsewhere (*38*), with the use of an affinity-purified mouse antiserum generated against purified p10 (*24*), and yielded punctate nuclear peripheral staining.
26. C. Strambio de Castillia, G. Blobel, M. P. Rout, *J. Cell Biol.* **131**, 19 (1995).
27. p10 (0.5 mg/ml) was dialyzed against 5 mM phosphate buffer (pH 6.0), added to a solution of 10-nm gold beads (pH 6.5) (Auro Beads G10, RPN476, Amersham) at a final concentration of 16 μg/ml, and left for 5 min at 20°C. Finally, the pH was adjusted to 9.0 and bovine serum albumin (BSA) was added to give a 1% final concentration. BSA-gold conjugates were prepared by means of the same protocol.
28. Nuclear envelopes were prepared from *S. uvarum* as described (*24*). Overlays were performed as described (*13*), except that dithiothreitol (DTT) was omitted from the washing buffer. p10-gold (*27*) was incubated with strips for 2 hours at 20°C at a 1-in-200 dilution in renaturing buffer (*13*) without DTT. For the competition experiment, p10 was added at a final concentration of 1.3 μM.
29. M. P. Rout and S. Wente, *Trends Biochem. Sci.* **4**, 357 (1994).
30. E. Coutavas, M. Ren, J. Oppenheim, P. D'Eustachio, M. Rush, *Nature* **366**, 585 (1993).
31. Nup36 is homologous to Nup2p and contains five FXFG peptide repeats, as well as a COOH-terminal RanBP1 homologous domain. Nup36 was localized to the NPC (U. Nehrbass and G. Blobel, unpublished results). ΔNup36, a truncated version of Nup36, lacks the COOH-terminal RanBP1 domain amino acids 208 to 327.
32. Yeast Ran was purified and preloaded with nucleotides as described previously (*20*). Kap60α and Kap95β were prepared as described elsewhere (*19*). Liquid phase binding assays were essentially performed as described (*19*).
33. In the absence of p10, no Ran-GDP was found in the bound fraction when added to docked karyopherin αβ. Use of GST-Nup1 (*19*) instead of GST-ΔNup36 gave similar results, in that Ran-GDP bound to docked karyopherin αβ in presence of p10. Accordingly, no Ran-GDP was found in the bound fraction in the absence of p10, as reported previously (*19*).
34. Amounts of Ran in the bound fraction, as judged by the apparent intensity of the silver-stained band, decreased to about 50% of the initial value after 1 hour of incubation with 200 μM GTP. Some GST-ΔNup36 appeared to bleed off the glutathione resin (*19*). This corresponded to a small amount of bound karyopherin bleeding into the nonbound fraction. In addition, some of the bound karyopherin β may dissociate from the p10-β-nucleoporin complex and appear in the nonbound fraction. The quantitative release of karyopherin α with most of karyopherin β remaining bound cannot be attributed to bleeding from the column.
35. This slight dissociation of both karyopherin α and β is likely to have been caused by small amounts of Ran-GTP that were present in the Ran-GDP preparation because of incomplete exchange. In the presence of p10, the contaminating Ran-GTP may not have been recruited into the pentamer and therefore might have been prevented from accessing the karyopherin heterodimer.
36. M. Peifer, S. Berg, A. B. Reynolds, *Cell* **76**, 789 (1994).
37. F. R. Bischoff, C. Klebe, J. Kretschmer, A. Wittinghofer, H. Ponstingl, *Proc. Natl. Acad. Sci. U.S.A.* **91**, 2587 (1994).
38. J. D. Aitchison, M. P. Rout, M. Marelli, G. Blobel, R. W. Wozniak, *J. Cell Biol.* **131**, 1133 (1995).
39. R. Rothstein, *Methods Enzymol.* **194**, 281 (1991).

40. We thank F. Kessler and J. Aitchison for helpful discussion and A. H. Brivanlou and F. Kessler for help in preparing the figures.

11 January 1996; accepted 4 March 1996